

Moist moss tundra on Kapp Linne, Svalbard is a net source of CO₂ and CH₄ to the atmosphere

Anders Lindroth¹, Norbert Pirk², Ingibjörg S Jónsdóttir³, Christian Stiegler⁴, Leif Klemedtsson⁵, and Mats B. Nilsson⁶

¹Lund University

²Department of Geosciences, University of Oslo

³Life and Environmental Sciences, University of Iceland

⁴University of Göttingen

⁵Goeteborg University, Sweden

⁶Swedish University of Agricultural Sciences

November 24, 2022

Abstract

We measured CO₂ fluxes which corresponds to a growing season estimate of 0.04 to 0.16 g CH₄ m⁻². We find that this moss tundra emits about 60 gCO₂-equivalents m⁻² yr⁻¹ of which CH₄ is responsible for 7%. Air temperature, soil moisture and greenness index contributed significantly to explain the variation in ecosystem respiration (R_{eco}) while active layer depth, soil moisture and greenness index best explained CH₄ emissions. Estimate of temperature sensitivity of R_{eco} and gross primary productivity showed that a modest increase in air temperature of 1 degree did not significantly change the NEE during the growing season but that the annual NEE would be even more positive adding another 8.5 gC m⁻² to the atmosphere. We tentatively suggest that the warming of the Arctic that has already taken place is partly responsible for the fact that the moist moss tundra now is a source of CO₂ to the atmosphere.

Hosted file

agusupporting-information_lindroth_v3.docx available at <https://authorea.com/users/551125/articles/604242-moist-moss-tundra-on-kapp-linne-svalbard-is-a-net-source-of-co2-and-ch4-to-the-atmosphere>

1
2 **Moist moss tundra on Kapp Linne, Svalbard is a net source of CO₂ and CH₄ to the**
3 **atmosphere**

4 **A. Lindroth¹, N. Pirk², I. S. Jónsdóttir³, C. Stiegler⁴, L. Klementsson⁵, and M. B.**
5 **Nilsson⁶**

6 ¹Department of Physical Geography and Ecosystem Science, Lund University, Lund, Sweden.

7 ²Department of Geosciences, University of Oslo, Oslo, Norway.

8 ³Life and Environmental Sciences, University of Iceland, Reykjavik, Iceland.

9 ⁴Bioclimatology, Georg-August Universität Göttingen, Göttingen, Germany.

10 ⁵Department of Earth Sciences, University of Gothenburg, Gothenburg, Sweden.

11 ⁶Department of Forest Ecology and Management, Swedish University of Agricultural Sciences,
12 Umeå, Sweden.

13 Corresponding author: anders.lindroth@nateko.lu.se

14
15 **Key Points:**

- 16 • A moist moss tundra in Svalbard is a small net source of CO₂ and CH₄ on an annual basis
- 17 • Temperature sensitivity during summer is higher for gross primary productivity than for
- 18 ecosystem respiration at low temperature (0-4.5 °C) and the opposite at higher
- 19 temperature
- 20 • A modest temperature increase of 1 degree increases ecosystem respiration and gross
- 21 primary productivity of similar magnitude during summer but strengthens the annual
- 22 source of CO₂
- 23 • Greenness index contribute significantly to explain variation in both carbon dioxide and
- 24 methane fluxes
- 25

26 Abstract

27 We used dark chamber measurements for CO₂ and CH₄ fluxes and eddy covariance for CO₂
28 fluxes to quantify the fluxes and to study their environmental controls from a moist moss tundra
29 in Svalbard. The net ecosystem exchange (NEE) during the summer (June-August) was on
30 average -0.40 g C m⁻² day⁻¹ or -37 g C m⁻² for the whole summer. Including also the spring and
31 autumn periods the NEE was reduced to -6.8 g C m⁻² and the annual NEE became positive, 15.2
32 gC m⁻² due to the losses during the winter. The CH₄ flux which was only measured during the
33 summer period showed a large spatial and temporal variability. The mean value of all 214
34 samples was 0.000511±0.000315 μmol m⁻²s⁻¹ which corresponds to a growing season estimate of
35 0.04 to 0.16 g CH₄ m⁻². Converting these emissions to CO₂-equivalents using a global warming
36 potential of 34 we find that this moss tundra emits about 60 gCO₂-equivalents m⁻² yr⁻¹ of which
37 CH₄ is responsible for 7%.

38
39 Air temperature, soil moisture and greenness index contributed significantly to explain the
40 variation in ecosystem respiration (R_{eco}) while active layer depth, soil moisture and greenness
41 index were the variables that best explained CH₄ emissions. Estimate of temperature sensitivity
42 of R_{eco} and gross primary productivity showed that a modest increase in air temperature of 1
43 degree did not significantly change the NEE during the growing season but that the annual NEE
44 would be even more positive adding another 8.5 gC m⁻² to the atmosphere. We tentatively
45 suggest that the warming of the Arctic that has already taken place is partly responsible for the
46 fact that the moist moss tundra now is a source of CO₂ to the atmosphere.

47 1 Introduction

48 Climate warming is predicted to be most evident at high latitudes (Friedlingstein et al., 2006)
49 with profound effects on ecosystem functioning. One of the high latitude regions that are
50 expected to experience the most dramatic changes caused by climate change is the Arctic. This
51 region which is located roughly north of the tree-line is characterized by cold winters and cool
52 summers and with mean annual temperatures below zero. The summer periods are short ranging
53 between 3.5 to 1.5 months from the southern boundary to the north and July is normally the
54 warmest month. Annual precipitation is generally low decreasing from about 250 mm in the
55 southern areas to 45 mm in polar deserts in the north (Callaghan et al., 2005).

56
57 The permafrost soils in the Arctic store 1035±150 Pg of organic carbon in the top 0-3 m
58 (Hugelius et al., 2014) which is more than the average 2010-2019 of 860 Pg of carbon in the
59 atmosphere (Friedlingstein et al., 2020). The increased warming in these areas can induce higher
60 decomposition rates due to increased microbial activity which will provide a positive feedback to
61 the climate system (Schuur et al., 2015). On the other hand, warming can also increase
62 photosynthesis and carbon uptake and thus compensate for, or exceed, the effect of increased
63 decomposition. Climate warming is also affecting plant community composition and the length
64 of the growing season (Post et al., 2009) which also has an impact on the processes regulating
65 annual carbon emissions and uptake (Bosiö et al., 2014). There is however a large uncertainty
66 regarding the timing, magnitude and possible sign of potential feedbacks caused by these
67 changes (Myers-Smith et al., 2020).

68
69 Understanding processes that are controlling the exchanges of greenhouse gases in the Arctic is
70 crucial for assessment of potential feedback effects. For this purpose, multiple year-around long-

71 term studies including direct measurements of CO₂ and CH₄ fluxes covering all seasons, winter,
72 spring, summer and autumn would be ideal. This is a great challenge in the harsh climate of the
73 Arctic and with limited support of key infrastructures for, e.g., provision of electricity for
74 operation of instruments.

75
76 In spite of these difficulties a few year-around studies have been performed during the last
77 couple of decades. In the low Arctic, Oechel et al. (2013) demonstrate the importance of the
78 wintertime fluxes in a tussock tundra ecosystem in Alaska. They found that the non-summer
79 season emitted more CO₂ than the corresponding uptake during the summer resulting in a net
80 source to the atmosphere of about 14 gC m⁻² on an annual basis. They also showed that the
81 shoulder seasons, spring and autumn roughly out-weighted the summer uptake. Euskirchen et al.
82 (2012, 2016) measured net CO₂ exchange in three different tundra ecosystems; heath tundra,
83 tussock tundra and wet sedge tundra in northern Alaska over three years. They found that the
84 uptake of -51 to -95 gC m⁻² during the summer (June-August) was overturned by the respiration
85 that occurred during the winter period resulting in net annual losses for all three ecosystems.
86 Zhang et al. (2019) reported five years of year-around flux measurements in a heath ecosystem
87 on west Greenland and they found that the heath was an annual sink of -35±15 gC m⁻². One year
88 with an anomalously deep snow pack showed a 3-fold higher respiration during the winter as
89 compared to the other years which resulted in a significantly lower net uptake during that year.

90
91 Even fewer studies have been done on year-around studies in the high Arctic. Lüers et al. (2014)
92 quantified the annual CO₂ budget using eddy covariance measurements in a river catchment area
93 near Ny-Ålesund on Spitsbergen in the Svalbard archipelago and they found that the ecosystem
94 was in C-balance. The footprint area was a semi-polar desert with only 60% vegetation cover and
95 patches of bare soil and stones. Also in Svalbard but further south in Adventdalen on a flat
96 alluvial fen irregularly covered with ice wedged polygons, Pirk et al. (2017) made year-around
97 measurements of CO₂ fluxes and found it to be a net sink of -82 gC m⁻². Because of the
98 irregularities caused by the ice wedges and the differences in wetness, they focused the analyses
99 on the spatial variability in two different directions, one wetter and one drier, and they estimated
100 the annual net ecosystem exchange to -91 gC m⁻² and -62 gC m⁻² for the respective areas.

101
102 The Arctic ecosystems constitute also a source of CH₄ to the atmosphere even if it is not a very
103 large one. Saunio et al. (2020) estimated that the Northern high latitude region (60°N - 90°N)
104 contributed 4% of global emissions and emissions from wetlands are only part of the emissions
105 from this region. However, in the light of the vulnerability of the high Arctic permafrost areas
106 and considering the large carbon pool and the predicted changes in climate, a quantification and
107 understanding of CH₄ exchanges in these areas are still important. Christensen et al. (2004)
108 showed one example of a dramatic impact of the climate warming on the CH₄ emissions in a
109 permafrost mire in sub-arctic Sweden. The warming which is visible in this area since decades
110 and its impact on permafrost and vegetation changes was estimated to have caused an increase of
111 landscape CH₄ emissions in the range 22-66% in the period 1970 to 2000.

112
113 Mastepanov et al. (2008) were the first to show the importance of emissions also outside of the
114 growing season. They observed a large burst of CH₄ from a fen area in Zackenberg, Greenland
115 after the growing season and during the time when the soil started to freeze. This finding was
116 confirmed in a later paper (Mastepanov et al., 2013) and the process was hypothetically

117 attributed to the subsurface CH₄ pool. Hydrology and vegetation composition play an important
 118 role for CH₄ emission and dynamics. McGuire et al. (2012) made a comprehensive summary of
 119 CH₄ exchanges of the Arctic tundra showing the difference between wet and dry ecosystems; the
 120 wet tundra emitted 5.4 to 13.0 gCH₄-C m⁻² during summer and 8.5 to 20.2 gCH₄-C m⁻² annually.
 121 The corresponding values for the dry/mesic tundra were 0.3 to 1.4 gCH₄-C m⁻² and 0.3 to 4.3
 122 gCH₄-C m⁻², respectively. Bao et al. (2021) utilized year-around measurements of CH₄ fluxes
 123 from three sites of the Ameriflux network in Northern Alaska to demonstrate the importance of
 124 the spring and autumn seasons for the annual emission. The shoulder seasons contributed about
 125 25% of the annual emissions and the autumn season had about three times higher emission than
 126 the spring season. These findings increasingly emphasise the importance of year-around
 127 measurements to fully understand the CH₄ controls and dynamics.

128

129 The main aim of this study is to provide another piece of the puzzle concerning CO₂ and CH₄
 130 exchanges from different but widespread ecosystem types in the high Arctic. We hypothesise
 131 that this moist tundra ecosystem is a net annual carbon sink and that the summer emissions of
 132 methane will be at average levels. We made flux measurements of CO₂ and CH₄ in a moist
 133 moss tundra ecosystem situated at Kapp Linne on the west coast of the Svalbard archipelago in
 134 2015 and with an additional campaign in 2016. The measurements in 2015 were done using both
 135 eddy covariance system (CO₂) and chambers (CO₂ and CH₄) but only chambers in 2016. We
 136 quantify ecosystem respiration (R_{eco}), gross primary productivity (GPP) and net ecosystem
 137 exchange (NEE) during the growing season based on measurements and we extend the time
 138 period to a full year by modelling. The CH₄ emission was only quantified for the summer season.
 139 We also analyze the environmental controls of the fluxes.

140 2 Materials and Methods

141 2.1 Research site and measurements

142

143 This study was performed in the Svalbard archipelago near the weather station Isfjord Radio
 144 (78°03'08"N 13°36'04"E, alt. 7 m) which is located right on the foreland of Kapp Linné on the
 145 island of Spitzbergen (Fig. S1). The tundra area where the measurements were performed is
 146 located about 1 km southeast of the station. The study area consists of moist moss tundra, a
 147 widespread ecosystem in Svalbard (Vanderpuyé et al., 2002; Ravolainen et al., 2020). The
 148 vegetation is characterised by the moss species *Tomentypnum nitens*, *Sanionia uncinata* and
 149 *Aulacomium palustre* and a sparse cover of vascular plants (20-40%), dominated by *Equisetum*
 150 *arvense*, *Salix polaris* and *Bistorta vivipara*. Other vascular plant species found in the plots:
 151 *Saxifraga cespitosa*, *Saxifraga oppositifolia*, *Silene acaulis*, and some grass species, most likely
 152 *Alopecurus ovatus* (previously *A. borealis*), and *Poa arctica*. The vegetation analysis was made
 153 from photographs of chamber location plots taken between 26 June and 2 July 2015 (see Figs.
 154 S4a-4y in Supplement).

155

156 The net ecosystem exchange of CO₂ was measured with an eddy covariance (EC) system located
 157 centrally on the moss tundra (78°03'28.6"N 13°38'40"E). The sonic anemometer (USA-1; Metek
 158 GmbH, Germany) was mounted on top of a tripod (see Fig. S1) at 2.7 m height. The CO₂ and
 159 H₂O concentrations were measured with an open path sensor (LI-7500; Li-Cor Inc., USA) placed
 160 just beneath the sonic and inclined about 30° pointing towards east. Radiation components,

161 incoming and outgoing short-wave and long-wave (CNR-4; Kipp & Zonen, the Netherlands)
162 were measured at 2.0 m height above ground with the sensor directed towards south. All sensors
163 were connected to a datalogger (CR-1000; Campbell Scientific, USA) which was powered by a
164 solar panel and a battery. The EC sensors were sampled and stored at 10Hz and all other sensors
165 were sampled at 0.1Hz with storage of 30 min mean values. These measurements were made
166 from 25 June to 17 September 2015.

167
168 The soil efflux of CO₂ and CH₄ was measured with a dark chamber connected to a gas analyzer
169 (Ultraportable Greenhouse Gas Analyzer; Los Gatos Research, USA) on 24 locations within the
170 EC average footprint area. A circular thin-steel frame, 15 cm in diameter and 15 cm high, was
171 inserted ca 5 cm into the ground in each location. The sharp edge of the frames made it easy to
172 insert them into the ground without damaging the vegetation and with minimal soil disturbance.
173 A picture was taken of each frame (see Supplement) for documentation of vegetation and for
174 calculation of different indexes. The chamber was also made from steel and it had a rubber seal
175 in the end facing the frame (Fig. S2) to make it air tight when mounted on the frame. The volume
176 of the chamber and the part of the frame raised above the surface was 5.3 L. A small fan was
177 installed inside the chamber to provide good mixing of the air during measurement. A small
178 weight (stone) was placed on top of the chamber during measurement to prevent it from moving
179 due to wind gusts. During concentration measurement air was circulated in a closed loop
180 between the chamber and the gas analyzer in ca. 10 m long 4 mm diameter polyethene tubes (see
181 Fig. S2). The air flow through the analyzer was ca 1.2 L min⁻¹. The chamber was ventilated in
182 the free air about 1 minute before each measurement which lasted for 5 minutes. The
183 concentrations were recorded and stored once per second by the gas analyzer. The time stamp of
184 the recorded data was used to identify measurement cycles for analysis of fluxes.

185
186 The chamber measurement positions were selected in the following way. The frames were
187 grouped in two sections, one north-east and one south-west of the flux tower since it was
188 expected that the main wind direction would be along that direction. Each group was then split
189 into three subsections with four measurement points within each one of them. The locations were
190 named S1:1-S1:4, S2:1-S2:4, S3:1-S3:4, N1:1-N1:4, N2:1-N2:4 and N3:1-SN3:4. The four
191 measurement points within each subsection were then placed along a transect with 3-4 m
192 between each point. This way it was possible to measure all four chamber locations without
193 having to move the whole measurement system. Chamber measurements were made in three
194 separate campaigns: mid-summer (26 June to 2 July 2015), late-summer (25-27 August 2015)
195 and early-summer (14-15 June 2016). Each location was measured three times during each one
196 of the three campaigns, a total of 216 measurements. Besides gas concentrations, also soil
197 temperature (5 cm), soil moisture (0-5 cm) and active layer depth was measured during each
198 campaign.

199
200 Meteorological data needed for analyses and gap-filling were obtained as follows: Hourly air
201 temperature and relative humidity from Isfjord radio, half-hourly global radiation from
202 Adventdalen, daily snow depth and ground ice conditions from Svalbard airport and monthly
203 precipitation from Isfjord radio and Barentsburg. The distance between the measurement site and
204 these stations are; Isfjord radio, 1 km, Barentsburg, 13 km, Svalbard airport, 46 km and
205 Adventdalen, 50 km. Data sources are given in Acknowledgement.

206

207 3. Data analysis

208
 209 The rawdata from the eddy covariance flux measurements were analysed using the Eddypro
 210 software version 6.1.0 (Li-Cor, 2016). Correction was made for the impact of the additional heat
 211 flux in the sensor path of the open path analyzer on the flux calculations according Burba et al.
 212 (2008). Gap filling during the measurement period was made using the REdDyProc online eddy
 213 covariance data processing tool developed at the Max Planck Institute for Biogeochemistry
 214 (Wutzler et al., 2018) without u^* correction since we could not identify any specific u^*
 215 threshold. Only data of highest quality, i.e. class=0 was retained for the gap filling and further
 216 analyses. Gap filling outside of the EC measurement period to obtain the carbon balance for a
 217 full year was made using empirical relationships for R_{eco} and GPP (see below).

218
 219 For flux footprint calculations the roughness length (z_0) is needed and it was calculated from the
 220 wind profile relationship in near neutral ($-0.01 < z/L < 0.01$) conditions:

$$221 \quad z_0 = \frac{z_m}{e^{(u(z) \frac{k}{u^*})}} \quad (1)$$

222 where z_m is measurement height, $u(z)$ is wind speed at height z , k is von Karman's constant and
 223 u^* is friction velocity. We used the flux footprint prediction (FFP) online tool by Kjun et al.
 224 (2015) to calculate the footprint climatology.

225
 226
 227
 228 The fluxes from the chamber measurements were estimated from the time change of the
 229 concentrations using linear regression. Every individual measurement was inspected and
 230 evaluated manually. These inspections showed that 50 seconds for CO_2 and 100 seconds for CH_4
 231 were optimal to obtain near perfectly linear responses a few seconds after the chamber had been
 232 placed on the frame. The slopes of the regressions were then used to calculate fluxes per unit
 233 surface area. The flux detection limits for CO_2 and CH_4 were calculated in the following way:
 234 first the peak-to-peak variation in the respective gases were determined when the chamber was
 235 ventilated in the free air and when conditions were steady. Then 20 sets of artificial 'fluxes' for
 236 each gas species were estimated based on 100 randomly generated concentrations for each data
 237 set. The peak-to-peak difference was used as seed (input) for the randomly generated values. The
 238 95% value of the distribution of these randomly generated fluxes was taken as the flux detection
 239 limit for the respective gas.

240
 241 The pictures of the vegetation inside of the chamber frames were analysed using the ImageJ
 242 (<https://imagej.net>) public domain software. The camera color channel information (digital
 243 numbers for Red (R), Green (G) and Blue (B) channels) was collected from the JPEG pictures.
 244 This type of pictures is for instance used in studies that are tracking the phenological
 245 development of vegetation (e.g. Richardson et al., 2009). The so-called green index (GI) is
 246 applied to detect differences in greenness of vegetation:

$$247 \quad GI = G/(R+G+B) \quad (2)$$

250 This index was also estimated for the central footprint area (100 m radius) of the flux
251 measurement location using a picture taken at 160 m above the altitude of the measurement area.

252 Forward stepwise linear regression (Sigmaplot 12.5) was used to analyze the dependency of the
253 CO₂ and CH₄ fluxes on environmental variables. We tested for air temperature (T_a), soil moisture
254 (θ), soil temperature (T_s), active layer depth (ALD), measurement location (S_{id}) and GI.

255
256 For gap filling of R_{eco} we only had access to air temperature with full annual coverage and, thus,
257 we could only use this driver for estimation of the R_{eco}. The measured chamber CO₂ fluxes were
258 fitted to the Lloyd & Taylor (1994) model with air temperature (T_a) as independent variable:

$$259 \quad FCO_2 = a \cdot e^{b\left(\frac{1}{56.02} - \frac{1}{T_a + 46.02}\right)} \quad (3)$$

260
261 During the EC measurement period (25 June to 17 September 2015) the GPP was estimated as:

$$262 \quad GPP = NEE_f - R_{eco} \quad (4)$$

263
264 Where NEE_f is the gap filled NEE according to Wutzler et al., (2018). This way R_{eco} and GPP
265 become consistent with the measured and gap filled NEE. For the time before and after this
266 period NEE was estimated as the sum of modelled R_{eco} and modelled GPP. The data for the GPP
267 model was derived from:

$$268 \quad GPP_m = NEE_m - R_{eco} \quad (5)$$

269
270 Where NEE_m is the measured net ecosystem exchange. The GPP_m was then fitted to a light
271 response function:

$$272 \quad GPP_m = c1 + c2 \cdot c3 / (c2 + R_g) \quad (6)$$

273

274 **4 Results**

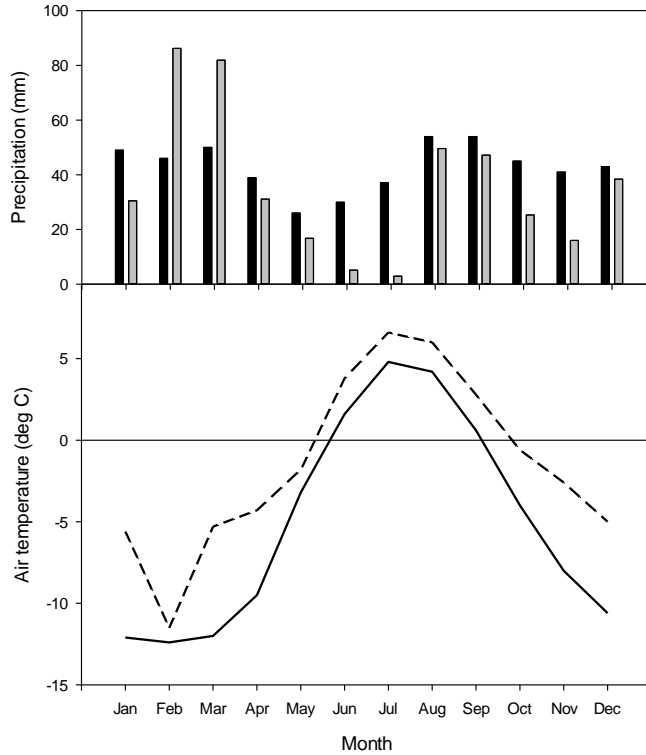
275 For CO₂ exchanges and partitioning we combined the soil efflux measurements with the chamber
276 system with the eddy covariance flux measurements. This was crucial for the partitioning and for
277 gap filling because from 20 April to 20 August at this location the sun is above the horizon 24
278 hours of the day and this means that there were few occasions of dark nighttime measurements
279 with the eddy covariance system and all of these were collected at the very end of the summer.
280 We consider the chamber measurements that were distributed across the summer to be more
281 representative of R_{eco} for this location.

282
283 For CH₄ exchanges we don't have any eddy covariance measurements so we present only
284 chamber data for this variable.

285 **4.1 Weather**

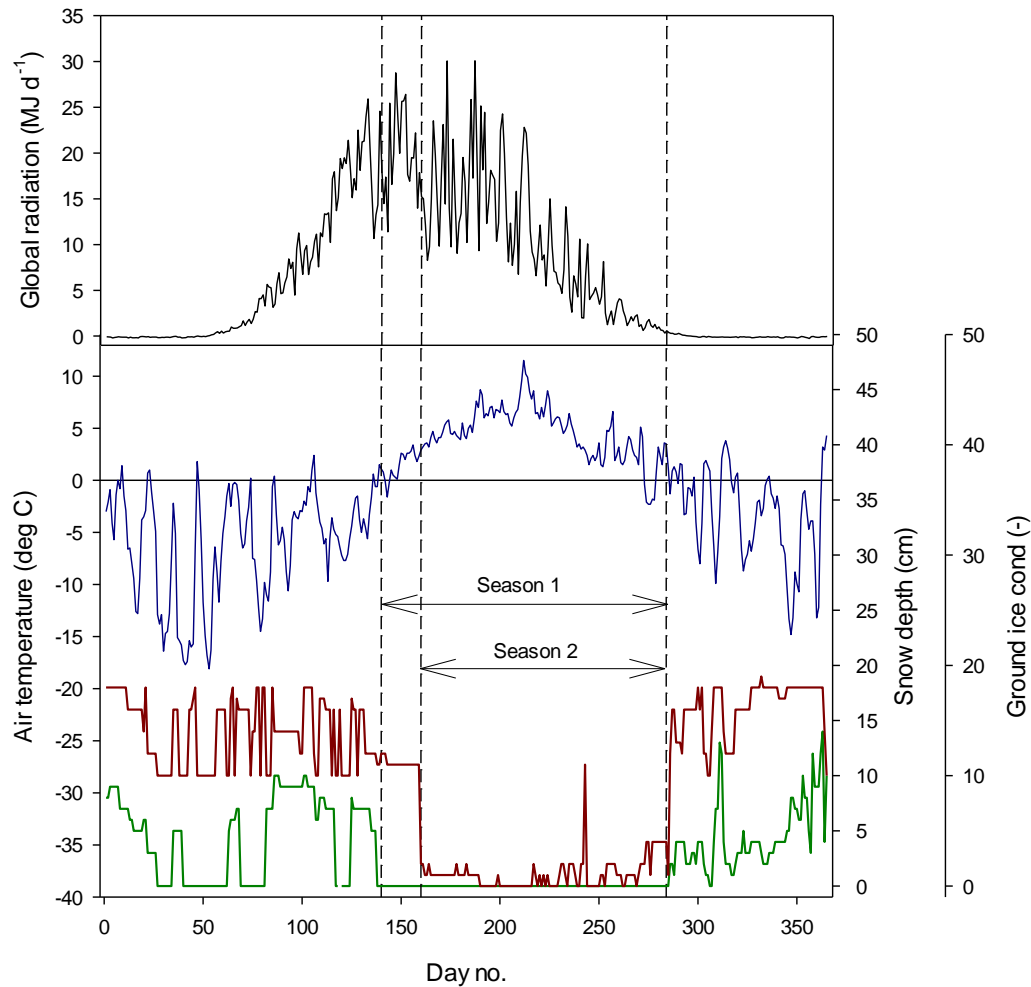
286
287 The mean annual temperature at Kapp Linne was -1.5 °C during 2015 which was 3.5°C higher
288 than the long-term mean (1961-1990) of -5.1 °C. The summer (June-August) mean of 5.5 °C was
289

294 2.0 °C higher than the long-term mean for the same time period (Fig. 1). The summer
 295 precipitation in 2015 was much lower, 58 mm as compared to the long-term precipitation which
 296 was 121 mm. The annual precipitation was also lower, 431 mm compared to the long-term
 297 precipitation which was 514 mm.



298 Figure 1. Monthly precipitation (top): Long-term average 1961-1990 black bars and 2015 grey
 299 bars. Data from Barentsburg for January-May, from Isfjord Radio for June-December. Mean
 300 monthly air temperature (bottom): Solid line is long-term average 1961-1990 and dotted line is
 301 2015. Data from Isfjord Radio which is located about 1 km west of the investigation area.
 302

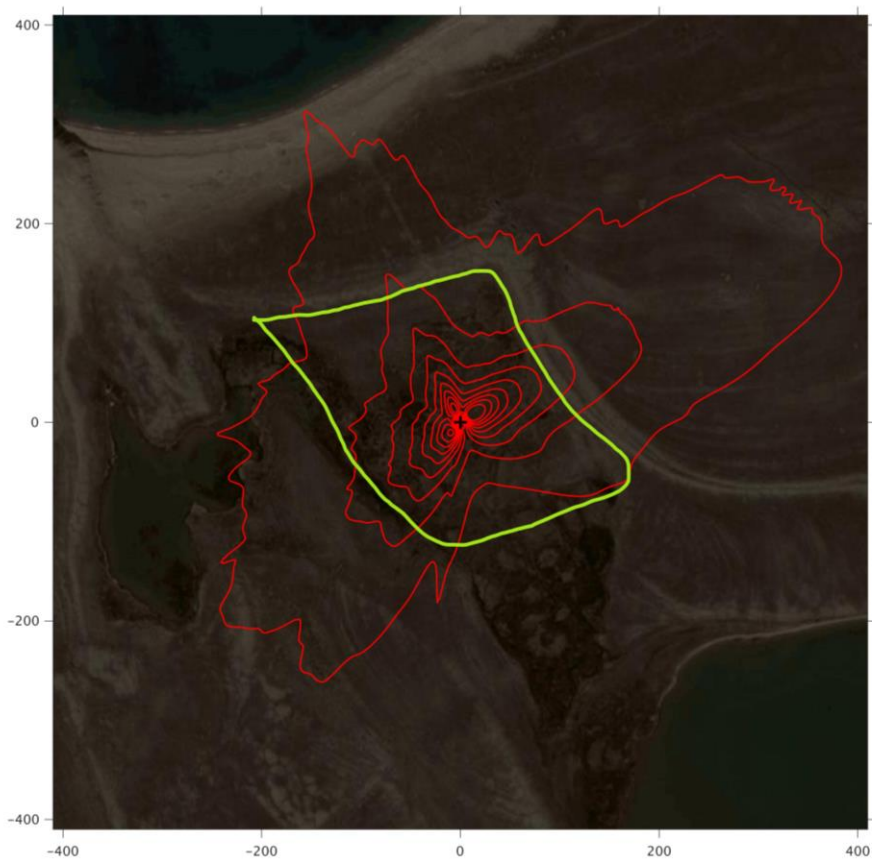
303 We defined the start of the growing season (the period during which vegetation is
 304 photosynthesizing) in two different ways. The first (denoted Season 1, day no. 140; see Fig. 2)
 305 based on when daily air temperature started to stay above zero more steadily and the second
 306 (denoted Season 2, day no. 160) when most of the snow had disappeared. The ending of the
 307 growing season was defined as when the air temperature fell more steadily below zero, when
 308 ground ice began to establish and when a significant snow pack was established (day no. 284;
 309 Fig. 2).
 310



311
 312 Fig. 2 Weather conditions during 2015. Top panel: Mean daily global radiation at Adventdalen.
 313 Bottom panel: Mean daily air temperature at Isfjord Radio (blue), snow depth (red) and ground
 314 ice conditions (green) at Svalbard airport close to Longyearbyen. The ground ice condition is
 315 scaled from 0 to 20 where 0 is no snow or ice on the ground and 20 indicate a complete cover of
 316 snow or ice.

317 318 4.2 Flux footprint and greenness

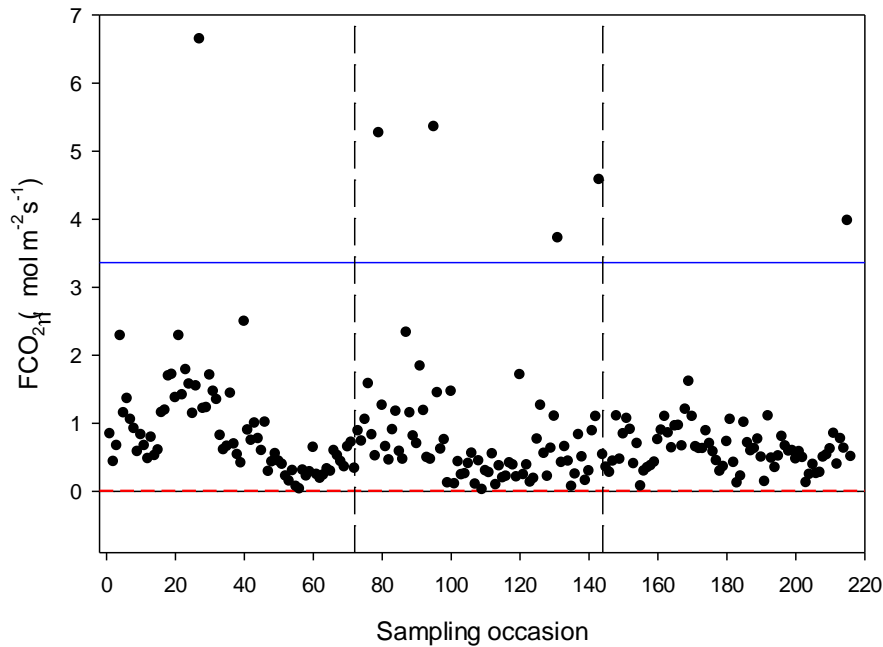
319
 320 The footprint climatology shows a good representativity of the moss tundra surface by the EC
 321 measurements with 60-70% of fluxes emanating from areas well within the border of the tundra
 322 (Fig. 3). The mean green index for a circular area with radius of 100 m centered at the flux tower
 323 was 0.34 which corresponded exactly to the mean value for all chamber locations. The GI for the
 324 24 chamber locations varied between 0.316 and 0.369. We observed a good (visual) correlation
 325 between GI and coverage of green plants (see Figures S4a-S4y of chamber location pictures and
 326 GI).
 327



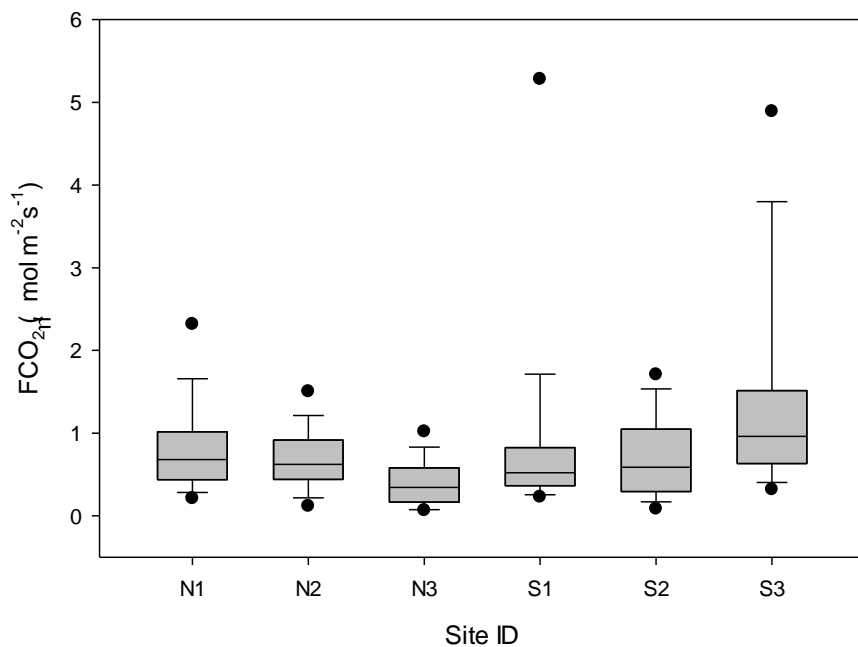
328
 329 Figure 3. The footprint climatology with red contour lines 10-90%. The area within the green
 330 line mark the heart of the moss tundra. The scale (m) is shown on the outer borders of the
 331 picture.

332 4.3 CO₂ exchanges

333
 334 The CO₂ fluxes from the chamber measurements showed quite large variation over time (Fig. 4)
 335 and across sampling locations (Fig. 5). The mean CO₂ flux of all samples was $0.81 \pm 0.11 \mu\text{mol}$
 336 $\text{m}^{-2}\text{s}^{-1}$. The uncertainty is given as the 95 confidence limit.
 337
 338



339
 340 Figure 4. Measured CO₂ exchange from the 24 sampling points using dark chamber and portable
 341 gas analyzer. The dashed red line indicates CO₂ flux detection limit and the blue line represents
 342 3xS.D. of all data points. The dashed vertical lines separate sampling periods from left to right:
 343 early summer, mid-summer and late-summer.



344
 345 Figure 5. Box plot of CO₂ fluxes per sampling location named N1-N3, S1-S3. The boundaries of
 346 the grey boxes represent the 25% and 75% percentiles, the line represent the median, whiskers
 347 above and below the boxes indicate the 10% and 90% percentiles. Outlying points are also
 348 shown.

349

350 Of the tested environmental variables T_a , θ , T_s , ALD, S_{id} and GI it was only T_a , θ and GI that
 351 contributed positively and significantly in decreasing order to explain the variability of the CO_2
 352 flux (Table 1).

353

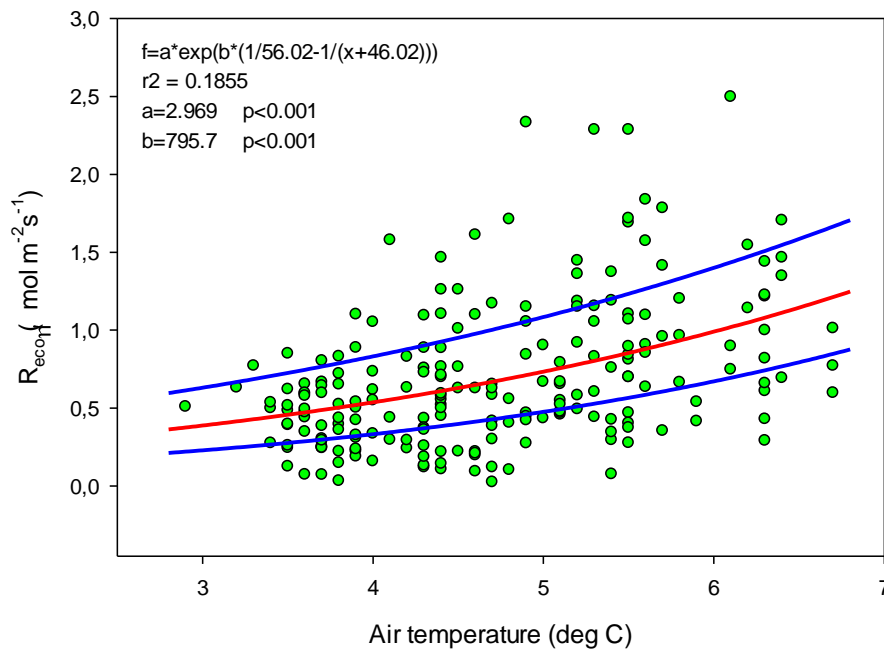
354 Table 1. Result of stepwise linear regression with CO_2 flux as dependent variable. Normality test
 355 failed but significance in all variables was confirmed with Wilcoxon Signed rank tests.

356

Variable	Partial- R^2	Probability (p)
T_a	0.190	<0.001
θ	0.037	0.002
GI	0.023	0.002

357

358 Ideally all of these variables should be used in a model to estimate R_{eco} for gap filling purposes
 359 but we could only use air temperature since this was the only variable that we had access to with
 360 complete coverage for a full year. The Lloyd & Taylor model (Eq. 3 & Fig. 6)) was thus used to
 361 estimate ecosystem respiration for 2015 using half-hourly air temperature as input.

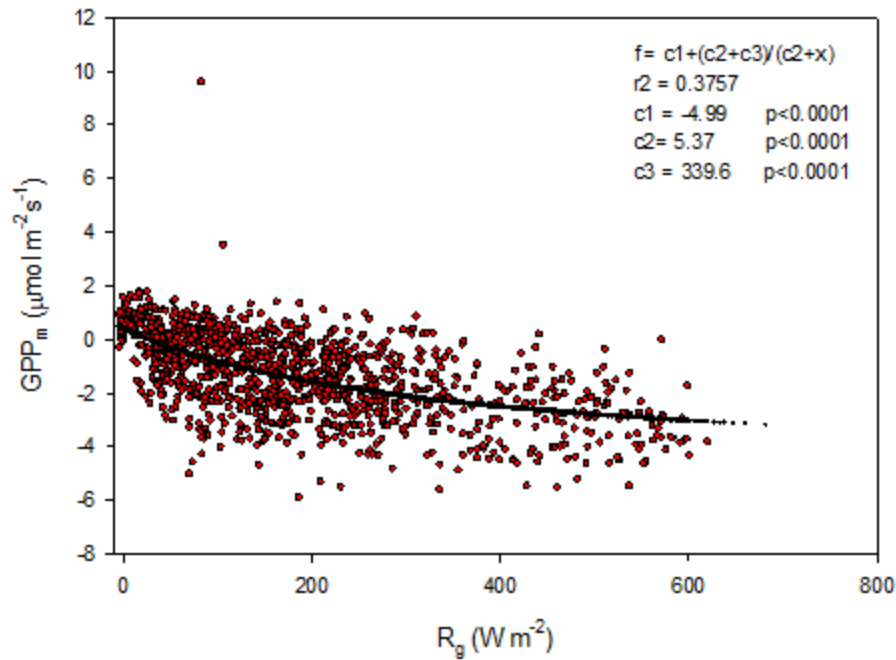


362

363 Figure 6. Measured ecosystem respiration (green dots) plotted against air temperature. The red
 364 curve is the fitted equation and the blue curves are the corresponding boundaries when
 365 considering the standard deviation of the parameters.

366

367 The modelled gross primary productivity (Eq. 6; GPP_m) had a small offset when global radiation
 368 was zero (Fig. 7). This offset was adjusted for when the model was applied for gapfilling so that
 369 GPP become zero during nighttime.



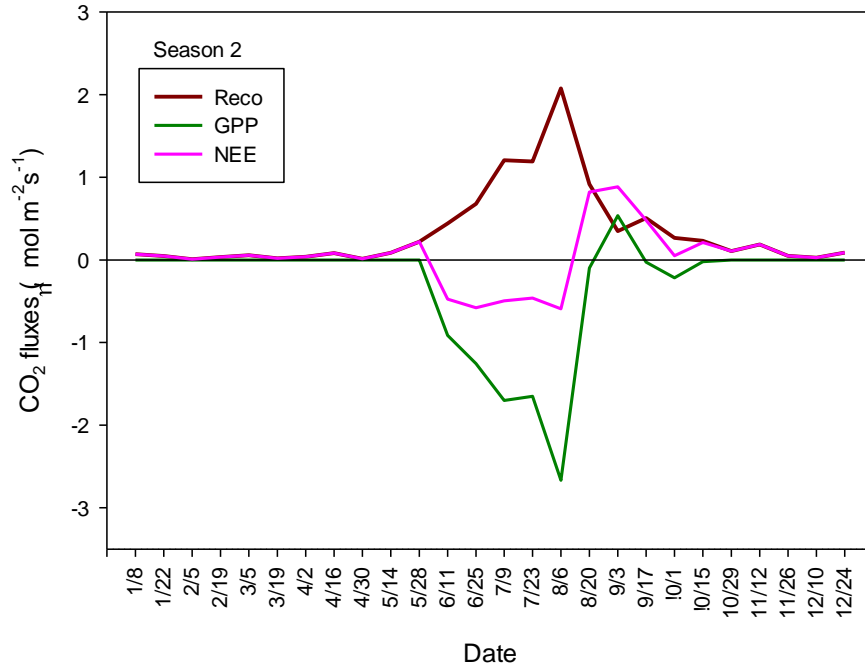
370
371

372 Figure 7. GPP_m plotted against global radiation; red symbols are estimated values according to
373 eq. (5) and the black symbols are the fitted model.

374

375 We assumed that GPP was zero for the periods outside of the growing season and that our R_{eco}
376 model was valid during winter as well as during growing season. The mean bi-weekly fluxes
377 show that NEE is negative from about one week into June until one week into August (Fig. 8).
378 The mean NEE is relatively constant during this period with a low $-0.5 \mu\text{mol m}^{-2}\text{s}^{-1}$. The
379 maximum bi-weekly GPP is about $-2.5 \mu\text{mol m}^{-2}\text{s}^{-1}$ while the corresponding R_{eco} is about 2.0
380 $\mu\text{mol m}^{-2}\text{s}^{-1}$. The GPP become positive during one period in the autumn indicating an
381 underestimation of R_{eco} during that time.

382



383
384 Figure 8. Bi-weekly gap filled CO₂ fluxes for season 2 (see Fig. 2) at Tunsjömyren, Kapp Linne
385 during 2015.

386
387 The annual modelled and gap filled NEE was negative, -25.3 gC m⁻² for season 1 and positive,
388 15.2 gC m⁻² for season 2. The gapfilled NEE (Table 2) during the summer (June-August) was -37
389 g C m⁻² or -0.40 g C m⁻² day⁻¹ which is good agreement with the measured NEE (25 June -31
390 August) with a mean daily uptake of -0.40 g C m⁻² day⁻¹. A summary of all components for the
391 different seasons are presented in Table 2.

392
393 Table 2. Summary of annual and seasonal C-fluxes from Kapp Linne.
394

Period	Component (gC m ⁻²)	Season	
		1	2
Winter	Reco	15.8	21.2
	GPP	0	0
	NEE	15.8	21.2
Growing season	Reco	114.9	109.5
	GPP	-156.8	-116.3
	NEE	-41.9	-6.8
Summer (June- August)	Reco	97.8	97.8
	GPP	-134.8	-134.8
	NEE	-37.0	-37.0
Annual	Reco	131.5	131.5
	GPP	-156.8	-116.3
	NEE	-25.3	15.2

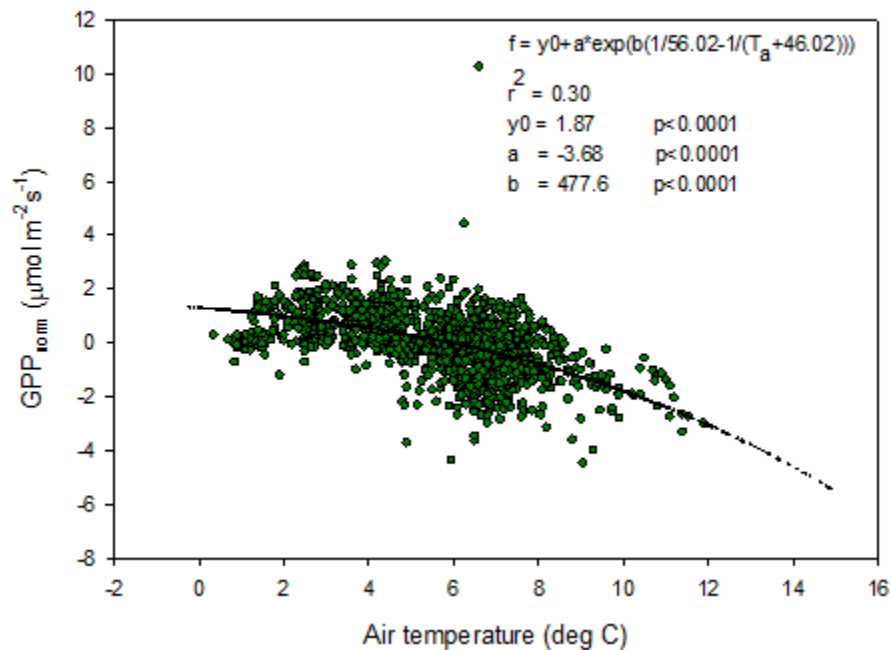
395

396

4.4 Temperature sensitivity of R_{eco} and GPP

397

398 The temperature sensitivity of the R_{eco} is already given by the fitted Lloyd & Taylor (1994)
 399 equation. In the absence of long time series of measurements during multiple year were natural
 400 climate variability could be used to assess temperature sensitivity of GPP we approached this
 401 problem in the following way. We normalize GPP for its dependence on radiation by estimating
 402 the difference between the ‘measured’ GPP and the model which only depends on radiation (see
 403 Fig. 7). The resulting normalized GPP show a dependence on air temperature (Fig. 9) with values
 404 becoming more negative with increasing temperature. We fitted the same type of model to these
 405 data as for the R_{eco} to be able to compare sensitivities to temperature.

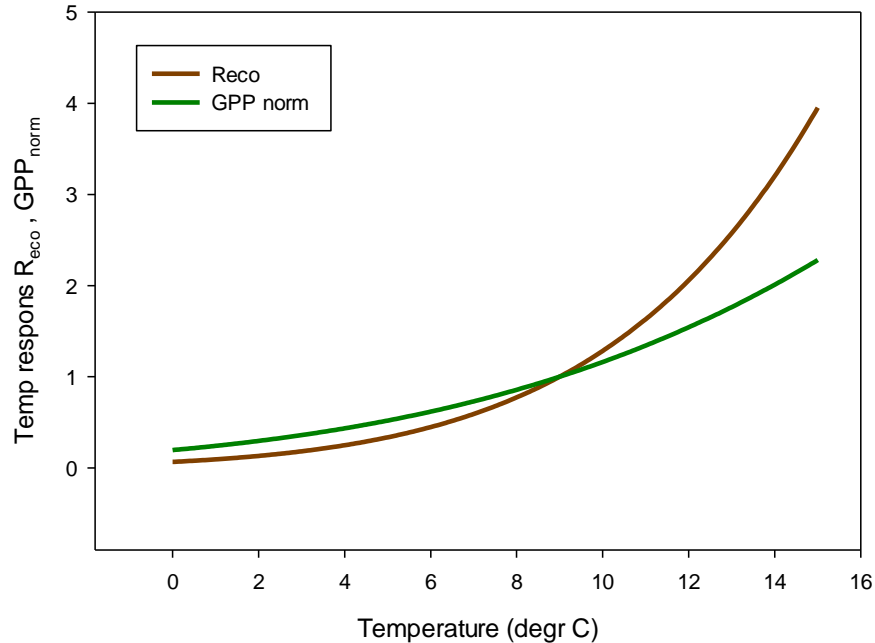


406

407

Figure 9. Normalized GPP plotted against air temperature and with the fitted exponential model.

408



409
410 Figure 10. Temperature sensitivity for R_{eco} (brown) and R_{g} -normalized (positive) GPP (green).
411

412 In Fig. 10 we reversed the sign of the GPP temperature response function to make it more easily
413 comparable with the R_{eco} response model. The temperature sensitivity ($\mu\text{mol m}^{-2}\text{s}^{-1}\text{K}^{-1}$) can be
414 estimated from the slope of these curves and the sensitivity is slightly higher for GPP than for
415 R_{eco} in the interval 0 – 4.5 °C, thereafter the difference is small up to about 7 °C then it began to
416 raise rapidly for R_{eco} . We tested what impact this could have by increasing the measured half-
417 hourly air temperature by 1 °C and found that during the growing season (season 2) the GPP
418 increased by -3.89 gC m^{-2} and R_{eco} by 3.53 gC m^{-2} . Thus, a minor increase of GPP compared to
419 R_{eco} . However, a one-degree higher winter temperature resulted in an addition respiration of 9 gC
420 m^{-2} . Thus, an estimated loss of 8.5 gC m^{-2} for the whole year.

421 422 4.5 CH₄ exchanges 423

424 The CH₄ fluxes from the chamber measurements showed large variation over time (Fig. 10) and
425 across sampling locations (Fig. 11). The mean CH₄ flux of all samples was 0.00051 ± 0.00024
426 $\mu\text{mol m}^{-2}\text{s}^{-1}$. The uncertainty is given as the 95% confidence limit. Setting all fluxes that fell
427 within the flux detection limits to zero changed the mean value with -0.2%. Assuming that the
428 mean flux was representative for the whole of growing season 1, the total CH₄ summer emission
429 was 0.039 to $0.164\text{ g CH}_4\text{ m}^{-2}$. Converting this to CO₂ equivalents (CO₂-eq; GWP=34) we get a
430 range of 1.3 to $5.6\text{ g CO}_2\text{-eq}$ for the summer and if we add also a possible winter emission of
431 22% of the annual (following Bao et al. 2021) we obtain an annual mean of $4.2 \pm 2.6\text{ g CO}_2\text{-eq}$.
432

433 We also noticed a clear trend during the summer with highest fluxes in mid-June and then
434 decreasing during the following two sampling occasions. The respective mean values with 95%
435 confidence intervals for the three sampling periods were $0.00121 \pm 0.000512\text{ }\mu\text{mol m}^{-2}\text{s}^{-1}$ (June 14-

436 15), $0.000332 \pm 0.000465 \mu\text{mol m}^{-2}\text{s}^{-1}$ (June 26- July 2) and $-0.00000781 \pm 0.0000936 \mu\text{mol m}^{-2}\text{s}^{-1}$
 437 1 (August 25-26).

438

439 For CH_4 exchanges we found *ALD*, θ and *GI* to contribute significantly to explain the variance of
 440 the flux (Table 3). The CH_4 flux responded negatively to increasing *ALD* and positively to θ and
 441 *GI*.

442

443 Table 3. Result of stepwise multiple linear regression with CH_4 flux as dependent variable.

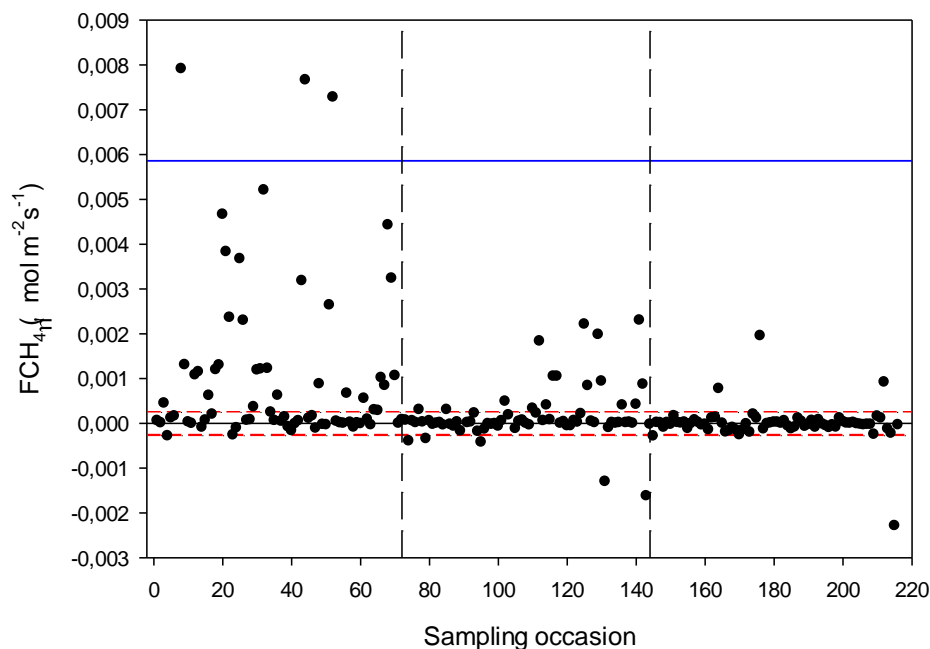
444 Normality test failed but significance in all variables was confirmed with Wilcoxon Signed rank
 445 tests.

446

Variable	Delta-R ²	Probability (p)
ALD	0.175	<0.001
θ	0.025	0.01
GI	0.020	0.004

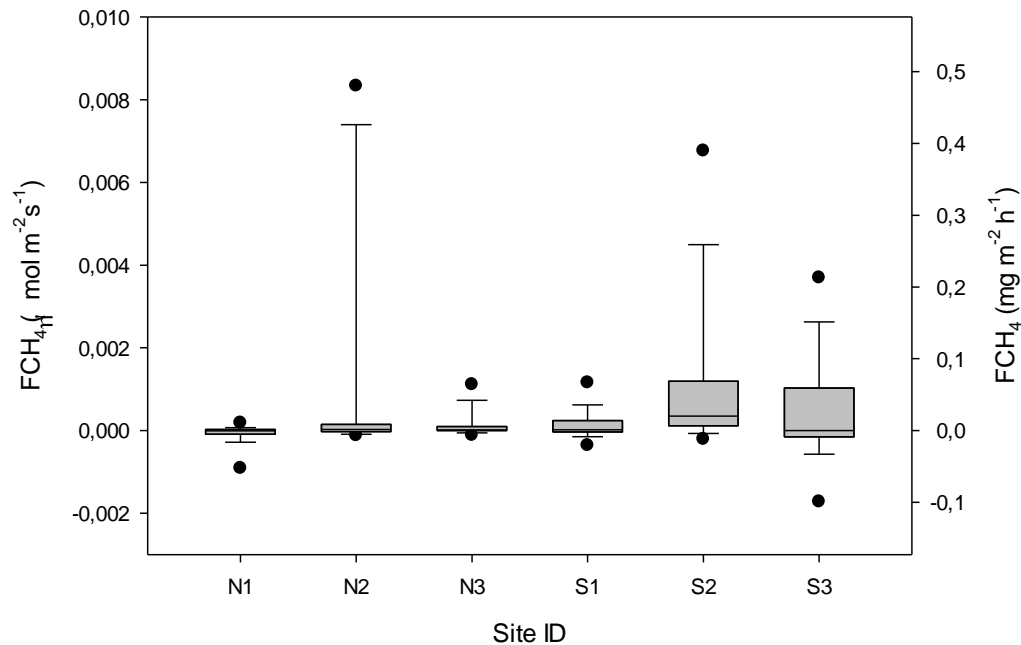
447

448



449

450 Figure 11. Measured CH_4 exchange from the 24 sampling points using dark chamber and
 451 portable gas analyzer. The dashed red lines indicate CH_4 flux detection limit, (i.e. inside the
 452 limits of detection the exact numbers are highly uncertain) and the blue line represents $3 \times \text{S.D.}$
 453 The dashed vertical lines – same as in Fig. 4.



454

455 Figure 11. Box plot of CH₄ fluxes per sampling location named N1-N3, S1-S3. The statistics
 456 includes also the data that fall within the flux detection limits. The boundaries of the grey boxes
 457 represent the 25% and 75% percentiles, the line represent the median, whiskers above and below
 458 the boxes indicate the 10% and 90% percentiles. Outlying points are also shown.

459 5 Discussion

460 5.1 Annual and seasonal CO₂ fluxes

461

462 We focus our discussion mainly on comparison with other tundra sites located in the North
 463 Atlantic area since these sites are influenced by the North Atlantic Current with its impact on
 464 weather patterns and climate. This limits the comparisons to sites in Greenland, Svalbard and
 465 Northern Scandinavia. However, we broaden the comparison a bit by adding two sites from
 466 Alaska.

467

468 Our annual NEE was in the range -25.3 to 15.2 gC m⁻² depending on definition of growing
 469 season (Table 2). We judge the latter value to be more realistic since season 1 includes an
 470 unrealistically high GPP when there is still a snow cover on the ground in early spring. Lund et
 471 al. (2012) found that the start of the uptake period was strongly correlated with start of the
 472 snowmelt for the fen in Zackenberg, NE Greenland. They defined the start of snowmelt as the
 473 day when snow depth was <0.1 m. This coincides very well with our definition of start of
 474 growing season 2 (see Fig. 2). Soegaard and Nordtroem (1999) reported an annual NEE of -64.4
 475 gC m⁻² for the fen in Zackenberg and Pirk et al. (2017) reported -82 gC m⁻² for an alluvial fen in
 476 Adventdalen, Svalbard, not far from Kapp Linne. For a site on the west coast of Greenland,
 477 Disco island with heath vegetation, Zhang et al. (2019) reported an annual NEE of -25±15 gC m⁻².
 478 Christensen et al. (2012) reported a range of -20 to -95 gC m⁻² for annual NEE in a palsa mire
 479 in Abisko, Northern Sweden. Our results are closer to the values found for a sparsely vegetated

480 catchment area in Bayelva, Ny-Ålesund were Lüers et al. (2014) reported annual NEE to be 0 gC
 481 m⁻². If we go beyond the North Atlantic area to the low Arctic region in North America we can
 482 find sites that has a positive NEE on annual basis, 13.6 gC m⁻² for a tussock tundra near
 483 Atquasuk, Alaska (Oechel et al., 2013) and 21-61 gC m⁻² for a heath and 2-82 gC m⁻² for a wet
 484 sedge ecosystem in Innavait creek (Eurkirchen et al., 2012).

485
 486 Lund et al. (2012) analysed 10 years of EC flux measurements from a heathland in Zackenberg
 487 and they reported a NEE range of -39.7 to -4.3 gC m⁻² for the growing season. Our result for the
 488 growing season NEE of -6.8 gC m⁻² (Season 2; Table 2) fall within the same range but it was
 489 only two years out of ten that showed that low uptake in Zackenberg heath. Their measured
 490 growing season GPP was in the range of -95.4 to -54.1 gC m⁻² and the R_{eco} was in the range of
 491 37.7 to 63.8 gC m⁻². Our corresponding values were -116.3 gC m⁻² for GPP and 109.5 gC m⁻² for
 492 R_{eco}. López-Blanco et al. (2017) presented data over a period of eight years of EC flux
 493 measurements from Kobbefjord, SW Greenland over an area of mixed fen and heath vegetation.
 494 Their growing season ranges were; for NEE -74.2 to -45.9 gC m⁻², for GPP -316.2 to -181.8 gC
 495 m⁻² and for R_{eco} it was 144.2 to 279.2 gC m⁻² excluding 2011 which was anomalous because of a
 496 pest outbreak and 2014 which did not have a full growing season.

497
 498 Our EC measurements of summer (June-August) NEE of -37 gC m⁻² (Table 2) is in-between
 499 ranges reported for fen type of vegetation in NE Greenland; -96.3 gC m⁻² (Soegaard and
 500 Nordstroem 1999) to -50 gC m⁻² (Rennermalm et al. 2005) and heath vegetation; -1.4 to -18.9 gC
 501 m⁻² (Groendahl et al. 2007).

502
 503 It is difficult to compare growing season values because they are rarely defined the same way.
 504 Only small differences in definition of start and end of growing season can have a large impact
 505 on the NEE values since NEE is the sum of two large components of almost equal size and of
 506 different sign. In our case a 20 days difference in the beginning of the season changes growing
 507 season NEE from -25.3 to 15.2 gC m⁻². It is also difficult to compare GPP and R_{eco} for any
 508 season since the methods to split NEE into components differ from case to case. The most
 509 reliable comparison is probably for summer season (June – August) since most studies represents
 510 this period best in terms of measurement coverage and quality. So, with this in mind we are
 511 pretty confident with placing the C-exchange rates of the moss tundra intermediate between fen
 512 and heath type of vegetation in the North Atlantic region.

513 514 5.2 CH₄ fluxes

515
 516 Our estimated growing season CH₄ flux of 0.08 gC m⁻² is very low compared to most other
 517 methane emitting tundra sites; the Zackenberg fen site emitted CH₄ in the range 1.4 to 4.9 gC m⁻²
 518 (Mastepanov et al. (2013), Jackowicz-Korczynski et al. (2010) reported 20.1 to 25.1 gCH₄ m⁻²
 519 for the Stordalen mire in Northern Sweden. For three different sites in northern Alaska, Bao et
 520 al. (2021) reported annual emissions between 1.8 and 8.5 gCH₄ m⁻² which corresponds to 0.94
 521 and 4.5 gCH₄ m⁻² for the growing season based on their estimate that growing season emissions
 522 are 52.6% of the annual emissions. Sachs et al. (2008) measured CH₄ exchanges with EC method
 523 in a northern Siberian polygon tundra and found generally low fluxes of about 18.5 mgCH₄ m⁻²
 524 day⁻¹ with little variation over the growing season. This rate adds up to 2.3 g CH₄ m⁻² for their
 525 four months long growing season.

526

527 It should be pointed out that we did not perform measurements during the shoulder seasons
528 meaning that we probably underestimate the seasonal total. Importance of shoulder seasons was
529 first pointed out by Mastepanov et al. (2008) which discovered a large burst of CH₄ at and after
530 the onset of soil freezing. One interesting observation is that the main part of our CH₄ flux
531 occurred during the sampling period 14-15 June 2016 which is about 30 days after snow melt.
532 This is the time of the season when CH₄ emissions normally are peaking (Mastepanov et al.
533 2013). After that, the rates dropped to practically zero in late August (see Fig. 10).

534

535 If we sum up the annual net CO₂ and CH₄ fluxes expressed as CO₂-eq we find that the moss
536 tundra is emitting in total 60 gCO₂-eq of which the methane stands for 7%. So even if the CH₄
537 fluxes are small, it still represents a significant global warming impact in relative terms.

538

539 The comparison between the different sites are hampered by the fact that they in most cases
540 belong to different bioclimatic subzones with differences in climate and vegetation (Walker et
541 al., 2005). The only site besides Kapp Linne that belong to subzone B is the one in Ny Ålesund.
542 The other high Arctic sites Adventdalen and Zackenberg both belong to subzone C, the
543 intermediate high/low Arctic sites Kobbefjord and Disco Island belongs to subzone D
544 respectively C/D. The low Arctic site Atqasuk belong to subzone D and the Imnavait Creek
545 belong to subzone E. The sub-Arctic Abisko is not classified by Walker et al. (2005) but based
546 mean July air temperature it should belong to subzone E. These differences in climate and
547 vegetation should be kept in mind when comparing results from different sites.

548

549 5.3 Environmental controls of fluxes

550

551 A key issue in high Arctic is how ecosystems with soil that contain large amounts of frozen
552 carbon will respond to warming. A recent report about the future climate of Svalbard (Hanssen-
553 Bauer et al. 2019) show that appalling changes are at risk to occur. By 2071-2100 compared to
554 1971-2000 the mean annual temperature is estimated to increase by 7 °C to 10 °C for the medium
555 and high emission scenarios, respectively. Precipitation is also estimated to increase by 45%
556 respectively 65% for these scenarios. Such large changes will of course also have a lot of other
557 impacts as well for instance shorter snow season, more erosion and sediment transport, changes
558 in vegetation composition and growth etc etc. Assessment of such large changes are very
559 difficult and is far beyond the scope of this paper. We have however shown that for a smaller
560 temperature increase of 1 degree, the impact on the net carbon balance during the growing
561 season will be minute; the increase in ecosystem respiration is compensated for by a
562 corresponding, or actually slightly larger increase of gross primary productivity. Similar
563 compensation effect was obtained for a heath site in Zackenberg by Lund et al. (2012). They
564 used multi-year measurements to assess the effect of changes in temperature on the growing
565 season fluxes. But, if we also consider an increase in temperature during winter, it is most likely
566 that the annual NEE becomes weakened. It is not unlikely that the impact of climate change with
567 higher temperature that is already a reality in Svalbard can be the reason why the annual NEE
568 now is positive, i.e. the moss tundra is a GHG source of CO₂ to the atmosphere.

569

570 We found that air temperature was the main control of ecosystem respiration followed by soil
571 moisture and greenness index (Table 1). We had expected that soil temperature should contribute

572 significantly to explain the variations in R_{eco} but it did not. Cannone et al. (2019) showed that
573 ground surface temperature at 2 cm depth contributed significantly to explain R_{eco} in nearby
574 Adventdalen during early, peak and late parts of the growing season. In their study soil moisture
575 was also significant during peak and late seasons. One possible explanation to this difference in
576 responses could be that our soil temperature was measured at 5 cm depth and that air temperature
577 was more representative for the microbial processes taking place in or near the soil surface.
578 Interestingly, GI contributed significantly to explain variations in R_{eco} . The GI was clearly
579 correlated with the abundance of *Salix polaris* (see Supplement) and thus we interpret the
580 positive correlation between GI and R_{eco} to be an effect of increasing contribution by autotrophic
581 respiration to the total respiration.

582 We found no significant correlation between CH_4 emission and temperature. The best
583 explanation was by active layer depth followed by soil moisture and GI (Table 3). But it should
584 be pointed out that ALD and θ are not independent from each other and that ALD can be
585 regarded as a proxy for any seasonal variability, like plant phenology. Soil moisture decreases
586 with increasing active layer depth. The correlation between GI and CH_4 emission is probably
587 also connected with abundance of *Salix polaris* which is a vascular plant. Vascular plants are
588 since long mentioned as a pathway for CH_4 from the soil interior to the atmosphere in wet tundra
589 ecosystems (e.g. Schimel 1995) but it could also be an effect of mediation of soil by the root
590 exudation of organic acids as mentioned by Ström et al. (2012). However, we have not found any
591 studies supporting the latter hypothesis concerning *Salix polaris*.

592 **6 Conclusions**

593 Our analyses of EC and chamber flux measurements have shown that the moss tundra on Kapp
594 Linne is a small source of CO_2 and an even smaller source of CH_4 on an annual basis.
595 Concerning the magnitude of the CO_2 exchanges during summer we find it to be in between
596 those of fens and heath ecosystems located in the North Atlantic region. The CH_4 exchange is
597 much lower than for other tundra ecosystems in the region.

598
599 The temperature sensitivity for CO_2 exchange was slightly higher for GPP than for R_{eco} in the
600 low temperature range of 0-4.5 °C, almost similar up to 7 °C and thereafter it was considerably
601 higher for R_{eco} . The consequence of this, for a small increase in air temperature of 1 degree (all
602 other variables assumed unchanged) was that the increases in the two fluxes practically evened
603 out during the growing season. But a warmer winter period would probably result in an increased
604 loss of carbon. We cannot rule out that the reason why the moss tundra is a net source today is an
605 effect of the warming that has already taken place in Svalbard.

606 The analysis of which environmental factors that controlled the small-scale fluxes showed that
 607 air temperature dominated for R_{eco} and active layer depth for CH_4 but we also found that
 608 greenness index significantly explained part of the variation in these fluxes. For R_{eco} we
 609 attributed this to an increased share of autotrophic respiration to the total and for CH_4 we
 610 hypothesized that the abundance of the woody shrub *Salix polaris* effected the exchange either
 611 through internal plant pathway for methane or through increased provision of C substrate to the
 612 anaerobic microbial community stimulating the production of methane. This finding is an
 613 indication that modeling of CO_2 as well as of CH_4 fluxes can be improved by also considering
 614 differences and changes in greenness of the vegetation.

615 **Acknowledgments, Samples, and Data**

616 This work did not receive any other funding except salaries for the authors from their respective
 617 organizations. Observations of air temperature, relative humidity, precipitation, ground ice
 618 conditions and snow depth were obtained from Norwegian Centre for Climate Services (NCCS)
 619 and provided under licence CC BY 4.0. Global radiation data from Adventdalen was obtained
 620 from the University Centre in Svalbard (UNIS). Thanks to associated professor Jonas Åkerman,
 621 Lund University for support with information about the site. Data can be obtained from
 622 <https://zenodo.org>.

623

624 **References**

- 625 Bao, T., Xu, X., Jia, G., Billesbach, D.P. & Sullivan, R.C. (2021). Much stronger tundra methane
 626 emissions during autumn freeze than spring thaw. *Global Change Biology*, 27, 376–387.
 627 [https://doi.org/ 10.1111/gcb.15421](https://doi.org/10.1111/gcb.15421)
- 628 Bosiö, J., Stiegler, C., Johansson, M., Mbufong, H. N. & Christensen, T. R. (2014). Increased
 629 photosynthesis compensates for shorter growing season in subarctic tundra—8 years of
 630 snow accumulation manipulations. *Climatic Change*, 127, 321–334.
 631 <http://doi.org/10.1007/s10584-014-1247-4>
- 632 Burba, G. G., McDermitt, D., Grelle, A., Anderson, D.J. & Xu, L. (2008). Addressing the
 633 influence of instrument surface heat exchange on the measurements of CO_2 flux from
 634 open-path gas analyzers. *Global Change Biology*, 14, 1854–1876.
 635 <https://doi.org/10.1111/j.1365-2486.2008.01606.x>
- 636 Callaghan, T.V., Björn, L O., Chapin III, F.S., Chernov, Y., Christensen, T.R., Huntley, B., Ims,
 637 R., Johansson, M., Jolly Riedlinger, D., Jonasson, S., Matveyeva, N., Oechel, W.,
 638 Panikov, N. & Shaver, G. (2005). Arctic tundra and polar desert ecosystems. In: ACIA
 639 (Ed.), *Arctic Climate Impact Assessment*, (pp. 243-352). Cambridge University Press.
- 640 Cannonea, N., Pontib, S., Christiansen, H.H., Christensen, T.R., Pirk, N. & Guglielmin, M.
 641 (2019). Effects of active layer seasonal dynamics and plant phenology on CO_2 land
 642 atmosphere fluxes at polygonal tundra in the High Arctic, Svalbard. *Catena*, 174, 142-
 643 153. [https://doi.org/ 10.1016/j.catena.2018.11.013](https://doi.org/10.1016/j.catena.2018.11.013)

- 644 Christensen, T.R., Johansson, T., Akerman, H.J. & Mastepanov, M. (2004). Thawing sub-arctic
645 permafrost: Effects on vegetation and methane emissions. *Geophysical Research Letters*,
646 31, L04501. <https://doi.org/10.1029/2003GL018680>
- 647 Christensen, T.R., Jackowicz-Korzynski, M., Aurela, M., Crill, P., Heliasz, M., Mastepanov, M.
648 & Friborg, T. (2012). Monitoring the Multi-Year Carbon Balance of a Subarctic Palsa
649 Mire with Micrometeorological Techniques. *Ambio*, 41, 207–217.
650 <https://doi.org/10.1007/s13280-012-0302-5>
- 651 Euskirchen, E. S., Bret-Harte, M. S., Scott, G. J., Edgar, C., & Shaver, G. R. (2012). Seasonal
652 patterns of carbon dioxide and water fluxes in three representative tundra ecosystems in
653 northern Alaska, *Ecosphere*, 3, 1–19. <https://doi.org/10.1890/ES11-00202.1>
- 654 Euskirchen, E.S., Bret-Harte, M.S., Shaver, G.R., Edgar, C.W., & Romanovsky, V.E. (2017).
655 Long-Term Release of Carbon Dioxide from Arctic Tundra Ecosystems in Alaska.
656 *Ecosystems*, 20, 960–974. <http://doi.org/10.1007/s10021-016-0085-9>
- 657 Friedlingstein, P., Cox, P., Betts, R., Bopp, L., von Bloh, W., Brovkin, V., Cadule, P., Doney, S.,
658 Eby, M., Fung, I., Bala, G., John, J., Jones, C., Joos, F., Kato, T., Kawamiya, M., Knorr,
659 W., Lindsay, K., Matthews, H. D., Raddatz, T., Rayner, P., Reick, C., Roeckner, E.,
660 Schnitzler, K. G., Schnur, R., Strassmann, K., Weaver, A. J., Yoshikawa, C., & Zeng, N.
661 (2006). Climate-carbon cycle feedback analysis: Results from the C4MIP model
662 intercomparison, *J. Climate*, 19, 3337–3353. <https://doi.org/10.1175/JCLI3800.1>
- 663 Friedlingstein, P., O’Sullivan, M., Jones, M.W. et al. (2019). Global carbon budget 2010. *Earth*
664 *Syst. Sci. Data*, 12, 3269–3340. <https://doi.org/10.5194/essd-12-3269-2020>
- 665 Groendahl, L., Friborg, T., & Soegaard, H. (2007). Temperature and snow-melt controls on
666 interannual variability in carbon exchange in the high Arctic. *Theor. Appl. Climatol.*, 88,
667 111–125. <http://doi.org/10.1007/s00704-005-0228-y>
- 668 Hanssen-Bauer, I., Førland, E.J., Hisdal, H., Mayer, S., Sandø, A.B. & Sorteberg, A. (2019).
669 Climate in Svalbard 2100 – a knowledge base for climate adaptation. *Report no. 1/2019*.
670 Norwegian Environment Agency.
- 671 Hugelius, G., Strauss, J., Zubrzycki, S., Haren, J.W., Schuur, E.A.G., Ping, C.-L., Schirrmeister,
672 L., Grosse, G., Michaelson, G.J., Koven, C.D., O’Donnell, J.A., Elberling, B., Mishra,
673 U., Camill, P., Yu, Z., Palmtag, J. & Kuhry, P. (2014). Estimated stocks of circumpolar
674 permafrost carbon with quantified uncertainty ranges and identified data gaps.
675 *Biogeosciences*, 11, 6573–6593. <http://doi.org/10.5194/bg-11-6573-2014>
- 676 Jackowicz-Korzynski, M., Christensen, T. R., Backstrand, K., Crill, P., Friborg, T.,
677 Mastepanov, M., & Strom, L. (2010). Annual cycle of methane emission from a subarctic
678 peatland. *J. Geophys. Res.-Biogeo.*, 115, G02009. <http://doi.org/10.1029/2008JG000913>

- 679 Kljun, N., Calanca, P., Rotach, M.W., & Schmid, H.P. (2015). A simple two-dimensional
680 parameterisation for Flux Footprint Prediction (FFP). *Geosci. Model Dev.*, 8, 3695-3713.
681 <http://doi.org/10.5194/gmd-8-3695-2015>
- 682 Li-Cor (2016). EddyPro® Software (Version 6.0) Li-Cor Inc., Lincoln, USA.
- 683 Lloyd, J., & Taylor, J.A. (1994). On the temperature dependence of soil respiration. *Functional*
684 *Ecology*, 8(3), 315-323.
- 685 Lopez-Blanco, E., Lund, M., Williams, M., Tamstorf, M.P., Westergaard-Nielsen, A., Exbrayat,
686 J.-F., Hansen, B.U., & Chrostensen, T.R. (2017). Exchange of CO₂ in Arctic tundra:
687 impacts of meteorological variations and biological disturbance. *Biogeosciences*, 14,
688 4467–4483. <https://doi.org/10.5194/bg-14-4467-2017>
- 689 Lund, M., Falk, J. M., Friborg, T., Mbufong, H. N., Sigsgaard, C., Soegaard, H., & Tamstorf, M.
690 P. (2012). Trends in CO₂ exchange in a high Arctic tundra heath, 2000–2010. *J.*
691 *Geophys. Res.- Biogeo.* <https://doi.org/10.1029/2011JG001901>
- 692 Lüers, J., Westermann, S., Piel, K., & Boike, J. (2014). Annual CO₂ budget and seasonal CO₂
693 exchange signals at a high Arctic permafrost site on Spitsbergen, Svalbard archipelago.
694 *Biogeosciences*, 11, 6307–6322. <http://doi.org/10.5194/bg-11-6307>
- 695 Mastepanov, M., Sigsgaard, C., Dlugokencky, E. J., Houweling, S., Strom L., Tamstorf, M. P., &
696 Christensen, T. R. (2008). Large tundra methane burst during onset of freezing. *Nature*,
697 456, 628–631. <http://doi.org/10.1038/nature07464>
- 698 Mastepanov, M., Sigsgaard, C., Tagesson, T., Ström, L., Tamstorf, M. P., Lund, M., &
699 Christensen, T. R. (2013). Revisiting factors controlling methane emissions from high-
700 Arctic tundra. *Biogeosciences*, 10, 5139–5158. <https://doi.org/10.5194/bg-10-5139-2013>
- 701 McGuire, A. D., Christensen, T. R., Hayes, D., Heroult, A., Euskirchen, E., Kimball, J. S.,
702 Koven, C., Lafleur, P., Miller, P. A., Oechel, W., Peylin, P., Williams, M., & Yi, Y.
703 (2012). An assessment of the carbon balance of Arctic tundra: comparisons among
704 observations, process models, and atmospheric inversions. *Biogeosciences*, 9, 3185–
705 3204. <https://doi.org/10.5194/bg-9-3185-2012>
- 706 Myers-Smith, I. H., Kerby, J. T., Phoenix, G. K., Bjerke, J. W., Epstein, H. E., Assman, J. J.,
707 John, C., Adreu-Hayles, L., Angers-Blondin, S., Beck, P. S. A., Berner, L. T., Bhatt, U.
708 S., Bjorkman, A. D., Blok, D., Bryn, A., Christiansen, C. T., Cornelissen, J. H. C.,
709 Cunliffe, A. M., Elmendorf, S. C., Forbes, B. C., Goetz, S. J., Hollister, R. D., de Jong,
710 R., Lorant, M. M., Marcias-Fauria, K., Maseyk, K., Normand, S., Olofsson, J., Parker,
711 T. C., Parmentier, F.-J. W., Post, E., Schaepman-Strub, G., Stordal, F., Sullivan, P. F.,
712 Thomas, H. J. D., Tømmervik, H., Treharne, R., Tweedie, C. E., Walker, D. A.,
713 Wilmking, M. & Wipf, S. (2020). Complexity revealed in the greening of the Arctic. *Nat.*
714 *Clim. Chang.*, 10, 106–117. <https://doi.org/10.1038/s41558-019-0688>

- 715 Oechel, W. C., C. A. Laskowski, G. Burba, B. Gioli, & Kalhori, A.A.M. (2014). Annual patterns
 716 and budget of CO₂ flux in an Arctic tussock tundra ecosystem. *J. Geophys. Res.*
 717 *Biogeosci.*, 119, 323–339. <http://doi.org/10.1002/2013JG002431>
- 718 Pirk, N., Sievers, J., Mertes, J., Parmentier, F.-J. W., Mastepanov, M., & Christensen, T. R.
 719 (2017). Spatial variability of CO₂ uptake in polygonal tundra: assessing low-frequency
 720 disturbances in eddy covariance flux estimates. *Biogeosciences*, 14, 3157–3169.
 721 <https://doi.org/10.5194/bg-14-3157-2017>
- 722 Post, E., Forchhammer, M. C., Bret-Harte, M. S., Callaghan, T. V., Christensen, T. R., Elberling,
 723 B., Fox, A. D., Gilg, O., Hik, D. S., Høye, T. T., Ims, R. A., Jeppesen, E., Klein, D. R.,
 724 Madsen, J., McGuire, A. D., Rysgaard, S., Schindler, D. E., Stirling, I., Tamstorf, M. P.,
 725 Tyler, N. J. C., van der Wal, R., Welker, J., Wookey, P. A., Schmidt, M. & Astrup, P.
 726 (2009). Ecological dynamics across the arctic associated with recent climate change.
 727 *Science*, 325, 1355–1358. <http://doi.org/10.1126/science.117311>
- 728 Ravolainen, V., Soininen, E. M., Jónsdóttir, I. S., Eischeid, I., Forchhammer, M., van der Wal,
 729 R. & Pedersen, A. Ø. (2020). High Arctic ecosystem states: Conceptual models of
 730 vegetation change to guide long-term monitoring and research. *Ambio* 49, 666–677.
 731 <https://doi.org/10.1007/s13280-019-01310-x>
- 732 Rennermalm, A.K., Soegaard, H., & Nordstroem, C. (2005). Interannual Variability in Carbon
 733 Dioxide Exchange from a High Arctic Fen Estimated by Measurements and Modeling.
 734 *Arctic, Antarctic, and Alpine Research*, 37(4), 545-556. [https://doi.org/10.1657/1523-
 735 0430\(2005\)037\[0545:IVICDE\]2.0.CO;2](https://doi.org/10.1657/1523-0430(2005)037[0545:IVICDE]2.0.CO;2)
- 736 Richardson, A. D., Braswell, B. H., Hollinger, D. Y., Jenkins, J. P. & Ollinger, S. V. (2009).
 737 Near-surface remote sensing of spatial and temporal variation in canopy phenology.
 738 *Ecological Applications*, 19: 1417–1428. <http://doi.org/10.1890/08-2022.1>
- 739 Sachs, T., Wille, C., Boike, J., & Kutzbach, L. (2008). Environmental controls on ecosystem-
 740 scale CH₄ emission from polygonal tundra in the Lena river delta, Siberia. *J. Geophys.*
 741 *Res.-Biogeosci.*, 113, G00A03. <http://doi.org/10.1029/2007JG000505>
- 742 Saunio, M., Stavert, A.R., Poulter, B et al. (2020). The global methane budget 2000-2017. *Earth*
 743 *Syst. Sci. Data*, 12, 1561–1623. <https://doi.org/10.5194/essd-12-1561>
- 744 Schimel, J.P. (1995). Plant Transport and Methane Production as Controls on Methane Flux from
 745 Arctic Wet Meadow Tundra. *Biogeochemistry*, 28 (3), 183-200.
 746 <https://doi.org/10.1007/BF02186458>
- 747 Schuur, E. A. G., McGuire, A. D., Schadel, C., Grosse, G., Harden, J. W., Hayes, D. J.,
 748 Hugelius, G., Koven, C. D., Kuhry, P., Lawrence, D. M., Natali, S. M., Olefeldt, D.,
 749 Romanovsky, V. E., Schaefer, K., Turetsky, M. R., Treat, C. C., & Vonk, J. E. (2015).
 750 Climate change and the permafrost carbon feedback. *Nature*, 520, 171–179,
 751 <https://doi.org/10.1038/nature14338>

- 752 Soegaard, H. & Nordstroem, C. (1999). Carbon dioxide exchange in a high-arctic fen estimated
 753 by eddy covariance measurements and modeling, *Glob. Change Biol.*, 5, 547–562.
 754 <https://doi.org/10.1111/j.1365-2486.1999.00250.x>
- 755 Strom, L., Tagesson, T., Mastepanov, M., and Christensen, T. R. (2012). Presence of
 756 *Eriophorum scheuchzeri* enhances substrate availability and methane emission in an
 757 Arctic wetland. *Soil Biol. Biochem.*, 45, 61–
 758 70.<http://doi.org/10.1016/j.soilbio.2011.09.005>
 759
- 760 Walker, D. A., Raynolds, M. K., Daniëls, F. J. A., Einarsson, E., Elvebakk, A., Gould, W. A.,
 761 Katenin, A. E., Kholod, S. S., Markon, C. J., Melnikov, E. S., Moskalenko, N. G., Talbot,
 762 S. S., Yurtsev, B. A. & the other members of the CAVM Team (2005). The Circumpolar
 763 Arctic vegetation map. *Journal of Vegetation Science*, 16, 267-282.
 764 <https://doi.org/10.1111/j.1654-1103.2005.tb02365.x>
 765
- 766 Vanderpuyve, A. W., Elvebakk, A. & Nilsen, L. (2002). Plant communities along environmental
 767 gradients of high-arctic mires in Sassendalen, Svalbard. *J. Veg. Sci.*, 13, 875–884.
 768 <http://doi.org/10.1111/j.1654-1103.2002.tb02117.x>
 769
- 770 Wutzler, T., Lucas-Moffat, A., Migliavacca, M., Knauer, J., Sickel, K., Šigut, L., Menzer, O.,
 771 Reichstein, M. (2018). Basic and extensible post-processing of eddy covariance flux data
 772 with REddyProc. *Biogeosciences*, 15(16), 5015-5030. Doi:10.5194/bg-15-5015-2018.
- 773 Zhang, W., Jansson, P-E., Sigsgaard, C., McConnella, A., Jammet, M.M., Westergaard-Nielsen,
 774 A., Lund, M., Friberg, T., Michelsen, A., & Elberling, B. (2019). Model-data fusion to
 775 assess year-round CO₂ fluxes for an arctic heath ecosystem in West Greenland (69°N).
 776 *Agricultural and Forest Meteorology*, 272-273, 176-186.
 777 <https://doi.org/10.1016/j.agrformet.2019.02.021>